Infrared quenching of persistent photoconductivity in GaAs/$Al_xGa_{1-x}As$ heterostructures

L. X. He
Department of Physics, University of Oregon, Eugene, Oregon 97403

K. P. Martin and R. J. Higgins
School of Electrical Engineering and Microelectronics Research Center, Georgia Institute of Technology, Atlanta, Georgia 30332
(Received 5 January 1988; revised manuscript received 11 July 1988)

Carrier number density and conductance measurements on GaAs/$Al_xGa_{1-x}As$ heterostructures for $2<T<77$ K confirm there is an infrared-induced (ir, $h\nu<0.7$ eV) quenching of persistent photoconductivity (PPC) in samples with $x=0.30$, 0.23, and 0.21. This is observed in both ungated and gated heterostructures with small gate biases. Measurements of de Haas–Shubnikov (dHS) oscillations show a decrease (relative to the PPC state) of the two-dimensional electron number density from the ir illumination, accompanied by increases in the dHS oscillation amplitude and the carrier scattering lifetime when the $Al_xGa_{1-x}As$ layer is not fully depleted. Together with shifts of the transconductance peak gate voltage and threshold voltage during ir quenching, the data establish that the decay in PPC is dominated by the capture of ir-excited free electrons back to deep centers in the $Al_xGa_{1-x}As$ layer. The capture-cross-section value estimated from the data is about 10^{-20} cm^2, which agrees with a calculation based on the energy of the ir-excited free electrons and the deep-trap-capture barrier height and decay prefactor. Data from gated samples show a gate electric field effect, where ir quenching (low electric fields) changes to ir enhancement (strong electric fields). This is discussed in terms of an electric-field-induced decrease in the optical threshold of emission from *DX* centers.

I. INTRODUCTION

Recently, we and others[1] have observed that while broadband white light ($h\nu>0.8$ eV) enhances conductivity in high-electron-mobility transistor (HEMT) structures, infrared light (ir, $h\nu>0.5$–0.8 eV), can erase a portion of the persistent-photocurrent effect (PPC) enhanced carrier density. An understanding of this phenomenon, known as infrared quenching (IRQ), helps resolve remaining puzzles of persistent photoconductivity and offers an opportunity for an intriguing application of PPC for optical information storage.

Nathan *et al.*[1] have observed infrared ($h\nu=0.6$–0.8 eV) quenching (as a 2% increase in the resistance) in an ungated GaAs/$Al_xGa_{1-x}As$ heterostructure sample ($x=0.3$) at 80 K. It was suggested[1] that this increased resistance occurs when the electrons are excited out of the high-mobility two-dimensional electron gas (2D EG) by absorption of the ir light and cross the barrier into the $Al_xGa_{1-x}As$ where they are recaptured. While the macroscopic barrier present in GaAs/$Al_xGa_{1-x}As$ heterostructures ordinarily prevents PPC-induced electrons at the 2D interface from rapid recapture by ionized donors in the $Al_xGa_{1-x}As$ layer, an ir-excited free electron can easily overcome this barrier (≈ 0.2 eV). The details were not explored in that work, but it may be noted that the photon energies where IRQ was observed (0.6–0.8 eV) were not sufficient to make electrons hop macroscopic recapture barriers (>0.8 eV) to recombine with holes in the epitaxially grown GaAs buffer layer or ionized impurities in the GaAs substrate.

Obviously free-carrier absorption of ir photons can occur in the Si-doped $Al_xGa_{1-x}As$ layer. But no reports have appeared that show significant infrared quenching of PPC in essentially "bulk" $Al_xGa_{1-x}As$ material which is generally grown on an undoped GaAs substrate and may actually be regarded as a GaAs/$Al_xGa_{1-x}As$ heterojunction with a thick (~ 1 μm) doped $Al_xGa_{1-x}As$ layer.[2] This weak ir response in "bulk" doped $Al_xGa_{1-x}As$ is consistent with the *DX*-center model shown in Fig. 1. The occupied *DX* center (trapped-carrier state) has an energy above the conduction band when at the configuration coordinate value where the unoccupied *DX* center (free-carrier state) sits with minimum energy. A valence electron, whose energy level is at least E_{gap} below the occupied *DX* center, cannot be optically transferred to a *DX* center by infrared light ($h\nu<E_{gap}$). However, as suggested by Nathan *et al.*, a conduction-band electron (i.e., unoccupied *DX*-center configuration) can be recaptured, forming an occupied *DX* center when the free electrons are excited by infrared light with photon energy E_1 smaller than the onset photon energy $E_{optical}$ (Fig. 1).

This *DX*-center filling mechanism is expected to be a relatively weak effect in bulk $Al_xGa_{1-x}As$ due to a conduction electron's small optical-absorption cross section (shown to be 10^{-19} cm^2 in the Appendix). The change in the $Al_xGa_{1-x}As$ carrier density (N_1) in HEMT structures is also expected to be small in measurements of the total sheet number density N_s or source-drain current, I_{SD} [Eqs. (1) and (2)]. The charge control model[3] and parallel conductance experiments[4] have shown that N_s and I_{SD} are dominated by the 2D EG density (N_{2D}) whose mobility is 100 times larger than carriers in the

$Al_xGa_{1-x}As$. However, a multiplier effect comes into play when the $Al_xGa_{1-x}As$ layer is depleted, and N_{2D} becomes sensitive to small changes in the ionized donor density of the doped $Al_xGa_{1-x}As$ layer (N_i). For example, a 1% decrease in a nominal 2×10^{17} cm^{-3} ionized donor density in a 100-nm-thick doped $Al_xGa_{1-x}As$ layer changes N_{2D} by 2×10^{10} cm^{-2} out of a total 4×10^{11} cm^{-2} (e.g., Fig. 2) or 5%, for a multiplier effect of 5. For HEMT samples with the gate voltage (V_g) near threshold (V_t), the multiplier effect can be much bigger because of the much smaller total N_{2D}. We propose that this is why IRQ is observed to be most significant for samples without free carriers in the $Al_xGa_{1-x}As$ layer.

The following sections explore several aspects of the capture of ir-excited free electrons. (i) When infrared light with $h\nu<0.65$ eV is used (thus avoiding contributions from the GaAs buffer layer and substrate), it is proposed that IRQ occurs by the capture of ir-excited electrons into traps in the doped $Al_xGa_{1-x}As$. Within this capture picture N_i decreases, with a corresponding decrease in N_{2D}. These changes in N_i and N_{2D} also change the 2D EG mobilities, which can be measured by either classical or quantum (de Haas–Shubnikov) methods.[5] (ii) The excitation is due to absorption of ir photons by free electrons. The capture cross section of ir-thermalized electrons trapped by deep levels must agree with the deep-trap-capture barrier heights and decay prefactors determined from independent thermal capture experiments. The discussion of part (ii) is left for Sec. VI. Experimental results from a variety of gated and ungated samples from different sources will be shown to be consistent with the above picture.

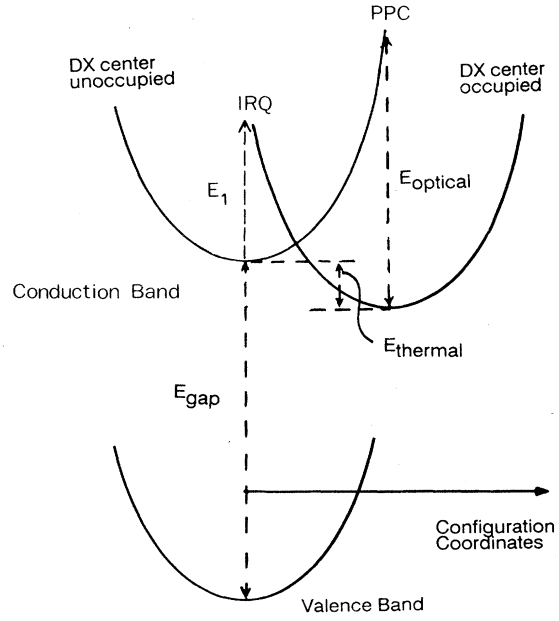

FIG. 1. The configuration coordinate model for a *DX* center. The figure shows the path for PPC onset and transition energy $E_{optical}$, as well as that for ir quenching and onset threshold, E_1.

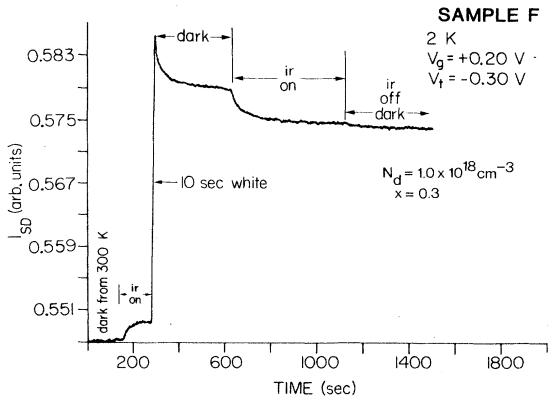

FIG. 2. Infrared-quenching: A typical source-drain current from sample F at 2 K under the influence of brief white-light and continuous ir illumination.

II. SAMPLES AND MEASUREMENTS

Most of the molecular-beam-epitaxy (MBE) grown heterostructures used in this work had the following layer sequence: Si-doped GaAs cap layer, Si-doped $Al_xGa_{1-x}As$ layer, undoped $Al_xGa_{1-x}As$ spacer layer, undoped GaAs buffer layer, and semi-insulating GaAs substrate. A 2D EG forms at the interface between the undoped $Al_xGa_{1-x}As$ and GaAs buffer layers, separated by the spacer layer from the nearest ionized donors in the $Al_xGa_{1-x}As$ layer. A typical device, the so-called high-electron-mobility transistor, has a metal gate on top of the GaAs cap layer with a length (L) to width (W) ratio $L/W>10$. Another type of device is a simple van der Pauw (VDP) square with an Ohmic contact in each corner.

Samples from four different MBE sources were used. Summarized in Table I are their principal parameters: aluminum fraction x, cap-layer thickness L_c, doping density $N_{d,c}$ of the cap layer, $Al_xGa_{1-x}As$ layer thickness L_a, $Al_xGa_{1-x}As$ layer doping density N_d, undoped spacer thickness L_s, gate voltage threshold (V_t) at 77 K in the dark, the net ionized donor density N_i in the depleted $Al_xGa_{1-x}As$ layer at 77 K in the dark, and the percentage increase of N_i after identical brief white light illumination sufficient to saturate the induced PPC. Samples A–C, E, and F were gated samples. Samples A, B, and G are on the same chip, but sample G is ungated. Samples A, B, F, and G had the same Al fraction ($x=0.3$) while samples C and E had $x=0.21$. Sample D, an ungated VDP, had $x=0.3$ in the doped $Al_xGa_{1-x}As$ layer but $x=1.0$ in the undoped spacer layer. Sample H is an ungated VDP square with $x=0.23$.

For gated HEMT samples, the source-drain current I_{SD} was measured with a fixed source-drain voltage (V_{SD}). For ungated Van der Pauw samples, N_s was measured via the Hall effect. When the 2D EG mobility (μ_{2D}) is much larger than the mobility of electrons in $Al_xGa_{1-x}As$ layer (μ_1) such that $\mu_1N_1 \ll \mu_{2D}N_{2D}$ (the difference between Hall mobility and conductance mobility is ignored because only the ratio μ_1/μ_{2D} is important

TABLE I. Principal sample parameters. Sample label, source, aluminum ratio x, cap-layer thickness L_c, doping density $N_{d,c}$ of the cap layer, $Al_xGa_{1-x}As$ layer thickness L_a, $Al_xGa_{1-x}As$ layer doping density N_d, undoped spacer thickness L_s, gate voltage threshold (V_t) at 77 K in the dark, the net ionized donor density N_i in the depleted $Al_xGa_{1-x}As$ layer at 77 K in the dark, and the percentage increase of N_i after identical brief white-light illumination sufficient to saturate the PPC-induced change. The layer thicknesses are in units of nm and doping or carrier densities are in units of 10^{17} cm^{-3}.

Sample	Source	x	L_c (nm)	$N_{d,c}$	L_a (nm)	N_d	L_s (nm)	V_t (V)	N_i	$\Delta N_i/N_i$
A,B	Tek[a]	0.3	50	2	100	10	5	−0.5	1.9	15%
C	TCSF[b]	0.21	20	6	120	6	8	−2.0	2.9	11%
D	Cornell[c]	0.3	20	10	30	10	10		ungated VDP	
G	Tek[a]	0.3	50	2	100	10	5		ungated	
E	TCSF[b]	0.21	20	6	120	6	8	−1.2	2.3	13%
F	Tek[a]	0.3	50	2	100	10	5	−0.2	1.6	20%
H	GE[d]	0.23	25	10	10	10	15		ungated VDP	

[a]Tek: Tektronix, Inc.
[b]TCSF: Thomson-CSF (Paris).
[c]Cornell: Cornell University.
[d]GE: General Electric Company.

in this case), N_s and I_{SD} can be written as

$$N_s = N_{2D} + 2N_1\mu_1/\mu_{2D} \quad (1)$$

(Hall measurement[6]) and

$$I_{SD} = -eGV_{SD}\mu_{2D}(N_{2D} + N_1\mu_1/\mu_{2D}) \quad (2)$$

(conductivity measurement) where G $(=W/L)$ is a geometrical factor for short-gate samples. In this study, $\mu_1 \approx 10^3$ cm^2/V sec while $\mu_{2D} \approx 10^5$ cm^2/V sec and N_1 never exceeds N_{2D} significantly, such that the condition for Eq. (1), $\mu_1 N_1 \ll \mu_{2D} N_{2D}$, is satisfied.

The ir light came from a white-light source filtered through a germanium lens with a cutoff at 0.67 eV. This is well below the onset optical threshold of 0.8 eV for PPC in $GaAs/Al_xGa_{1-x}As$ heterostructures.[1] Infrared quenching of PPC was observed for $2 < T < 77$ K in all samples. Figure 2 shows a sequence of I_{SD} versus time and light exposure where sample F has first been cooled from 300 to 2 K in the dark. The initial response to ir light is a weakly enhanced conductivity, in contrast to the larger increase in I_{SD} from white-light illumination. When the white light was removed, I_{SD} approaches a base line far above the initial in-dark value following an initial fast decay. After this, exposure to infrared illumination partially quenches the PPC enhancement of I_{SD}. Under steady ir illumination the quenching begins

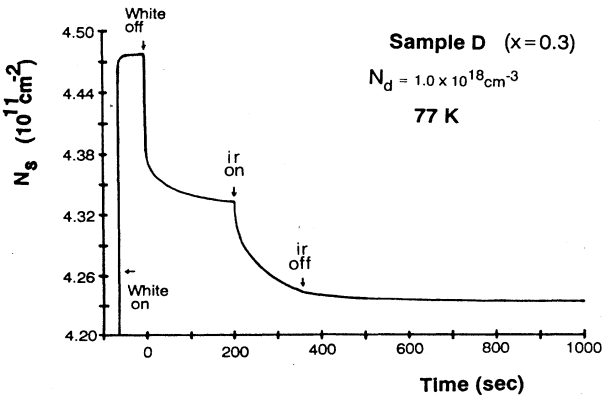

FIG. 3. Measurement of N_s during ir quenching in sample D.

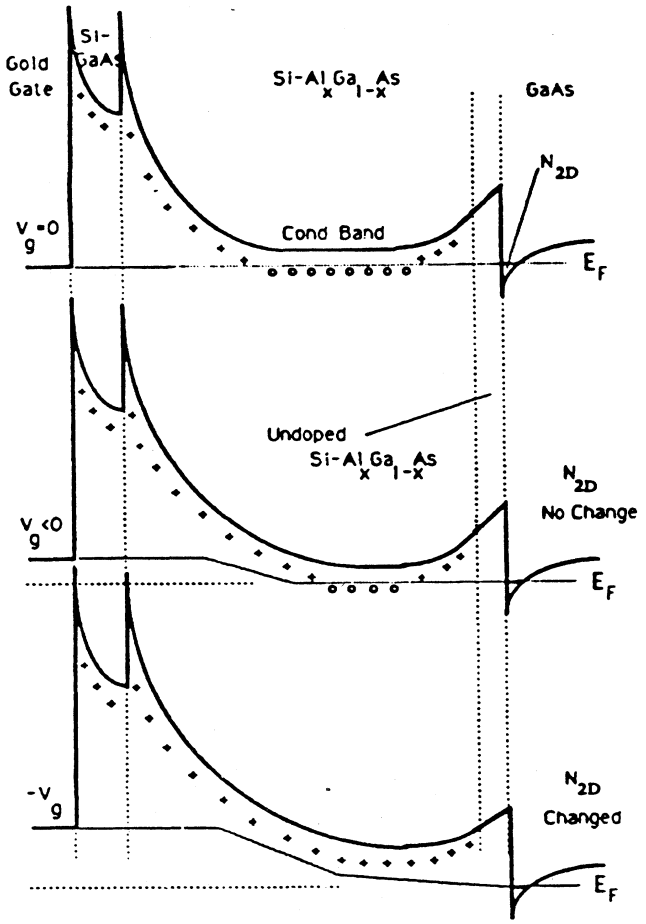

FIG. 4. The conduction-band bending in different layers of a HEMT device under different gate biases, going from (top) parallel conductance in the $Al_xGa_{1-x}As$ layer ($V_g=0$) to (bottom) full depletion in the $Al_xGa_{1-x}As$.

with a fast relaxation that slows as it approaches a base line value. For later times at these temperatures I_{SD} remains virtually unchanged after ir illumination is removed.

The base line value from IRQ does *not* depend on the illumination intensity. But the quenching decay time is strongly dependent on the ir light intensity. For example, when the ir intensity was increased by a factor of 10, the quenching time to the base line value was also reduced by a factor of 10.

At 77 K IRQ decreases N_s by 2% in sample D (Fig. 3) and 5% in sample H. For HEMT samples with V_g set so there is parallel conductance in the $Al_xGa_{1-x}As$ layer from low-mobility carriers [Fig. 4, (top)], the relative decrease of I_{SD} from IRQ is $\sim 1\%$. But when V_g is set close to V_t and only the 2D EG remains [Fig. 4, (bottom)], IRQ reduces I_{SD} by more than a factor of 10.

III. INFRARED QUENCHING OF PERSISTENT PHOTOCONDUCTIVITY

Since ir quenching reduces I_{SD} (Fig. 2), it is clear that the mechanism does not transfer electrons from the $Al_xGa_{1-x}As$ layer to the 2D interface, since $\mu_{2D} \gg \mu_1$ so I_{SD} would increase rather than decrease. To determine the net change in carriers in the $Al_xGa_{1-x}As$ layer, information other than simply the change in the source-drain current or overall sheet number density is required.

A. Transconductance of gated samples

For the gated depletion mode devices used, the conduction band bending across the $Al_xGa_{1-x}As$ layer was changed by varying the gate bias (Fig. 4). According to the charge control model for HEMT devices,[3,7] initial decreases (more negative) in V_g reduce the conductance of the $Al_xGa_{1-x}As$ layer while N_{2D} remains unchanged. When all carriers in the $Al_xGa_{1-x}As$ layer are depleted by V_g, N_{2D} begins decreasing with further lowering of V_g until channel pinchoff occurs. From this picture of charge control, the transconductance ($g_m = dI_{SD}/dV_g$) shows low values in the range of V_g which controls just the low-mobility carriers in the $Al_xGa_{1-x}As$ layer, but reaches much higher values when the gate bias controls the high-mobility 2D EG. When the transconductance is measured from $V_t < V_g < 0$, the g_m peak occurs at $V_g = V_p$, just past the point of $N_1 = 0$, and V_t occurs when N_1 and N_{2D} have been depleted. Therefore, shifts of V_p and V_t during thermal or optical processes provide important information about the carrier density changes in different heterostructure layers.

Figure 5 shows the following sequence of transconductance curves for sample A at 77 K: (1) sample initially in the dark, (2) after 30 sec of exposure to white light, (3) 1 min after removing the white light, and (6) after 2 min of infrared-light exposure. In addition, portions of the transconductance peak are shown (4) immediately after ir illumination begins and (5) 30 sec later during IRQ. The data in Fig. 5 show a shift of V_p from -0.15 to -0.42 V when going from the dark state to a fully saturated PPC state. V_p relaxes back to -0.38 V after the light is removed and then shifts further to -0.28 V upon receiving

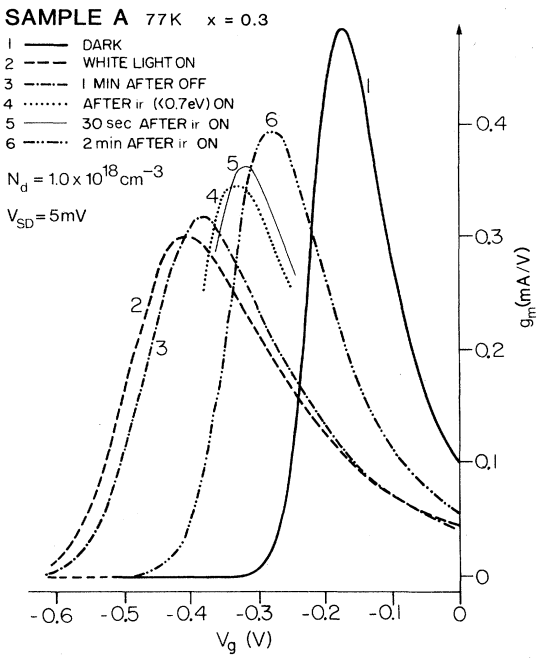

FIG. 5. Typical transconductance peak shifts under the influence of brief white light and continuous ir illumination from sample A at 77 K.

infrared illumination. V_t shows similar behavior. The relative difference between V_t and V_p also changes during these processes (0.13 V in dark, 0.17 V with white light on, and 0.15 V after IRQ), which indicates changes in depletion of the 2D EG. The change in N_1 at $V_g = 0$ is estimated from shifts of V_t or V_p by assuming the capacitance to be $C \approx \epsilon A/d$.[3] For sample A $\epsilon = 13$ is the dielectric constant, $A = 3 \times 10^{-6}$ cm^2 the area of gate, and $d = 150$ nm the distance between the gate and 2D EG interface with the result $C = 0.3$ pF. From $\Delta Q = C\,\Delta V_t$, there is a 3×10^{16}-cm^{-3} increase in N_1 upon white-light illumination, and a 1×10^{16}-cm^{-3} decrease upon ir illumination, for a 100-nm-thick doped $Al_xGa_{1-x}As$ layer. The estimated changes in N_1 (+3% with white light on, -1% after IRQ) are consistent with the relative changes in I_{SD} (+6% with white light on, -1% after IRQ) compared to $N_d = 1 \times 10^{18}$ cm^{-3} for HEMT samples with large parallel conductance in the $Al_xGa_{1-x}As$ layer (Fig. 2).

A factor of 2 decrease in the g_m peak amplitude is observed in the PPC state followed by the recovery of higher g_m values with IRQ (Fig. 5). This is evidence for N_i increasing in the PPC state and decreasing from IRQ. Screening effects are of secondary importance since N_{2D} only changes by a few percent.

Sample E with a lower in-dark threshold voltage of -1.2 V at 77 K shows a similar pattern: V_p shifted from -1.1 V (in dark) to -1.4 V (white light) and later decays to -1.35 V during the relaxation following white-light illumination and shifts further to -1.15 V upon exposure to infrared illumination.

The behavior of the transconductance permits us to conclude unambiguously that the free-carrier density or

the ionized donor density in the $Al_xGa_{1-x}As$ layer increases upon white-light illumination but later decreases upon receiving ir illumination.

B. de Haas–Shubnikov oscillations

Considerable evidence of the proposed ir-quenching mechanism was also accumulated from the de Haas–Shubnikov (dHS) measurements. The dHS oscillation amplitude σ_{OSC} at low magnetic fields measures the 2D EG mobility μ_{2D} ($=e\tau_q/m^*$) since

$$\sigma_{OSC}=C(B,T)[\sigma_{xx}(B=0)]\tau_q^2\exp(-\pi/\omega_c\tau_q) , \quad (3)$$

if $\omega_c\tau_q<1$.[8] In Eq. (3), ω_c is the cyclotron frequency, $\sigma_{xx}(B=0)$ the conductivity at zero magnetic field, $C(B,T)$ a weak function of B and temperature, and τ_q the quantum lifetime (Landau-level broadening), which is related to the classical Drude lifetime τ_c by[5]

$$\tau_q/\tau_c=(\pi/4)\tan(\beta/2) , \quad (4)$$

where $\beta=\pi/N_h$ and N_h is the Landau index.[9] For the samples in this work, N_h is about 10, so $\tau_q/\tau_c\approx 0.11$. The ratio τ_q/τ_c is not significantly changed during ir quenching so that the change of τ_c is proportional to that of τ_q.

For a short-gated sample, $\sigma_{xx}(B)$ is directly measured from I_{SD}.[10] For the VDP samples, $\sigma_{xx}(B)$ is calculated from measured values of the resistivities $\rho_{xx}(B)$ and $\rho_{xy}(B)$ by the relation

$$\sigma_{xx}(B)=\rho_{xx}(B)[\rho_{xx}^2(B)+\rho_{xy}^2(B)]^{-1} . \quad (5)$$

Figure 6 shows an example of the dHS oscillations from sample C at 2 K in the following sequence: in dark, after white light, and after IRQ. Shifts in both amplitudes (σ_{OSC}) and periodicity (N_{2D}) are visible. The 100% increase of σ_{OSC} after IRQ is accompanied by a 6% decrease of N_{2D}. This is different from a sample in the dark exposed to white light, which involves macroscopic PPC effects from the GaAs buffer layer; in that case both N_{2D} and σ_{OSC} increase (Fig. 6 where N_{2D} increases by 20%).

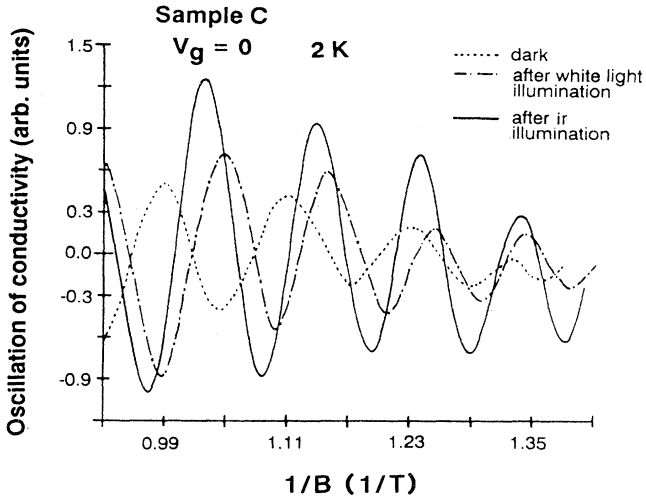

FIG. 6. de Haas–Shubnikov oscillations in the magnetoconductivity from HEMT sample C ($V_g=0$) at 2 K in the illumination sequence of dark, after white light exposure and after ir quenching.

The quantum lifetime is measured by fitting the oscillation amplitude to the leading exponential term in Eq. (3). Typical values of τ_q after ir quenching are

$$\tau_q=2.8\times10^{-13} \text{ sec (sample C)} ,$$

$$\tau_q=3.8\times10^{-13} \text{ sec (sample H)} .$$

dHS measurements complement bulk I_{SD} and N_s measurements since they single out N_{2d} and μ_{2D} at any point during PPC or IRQ, independent of the charge state of the parallel $Al_xGa_{1-x}As$ layer. Suppositions inferred from models or bulk transport can be checked independently.

The relative changes of N_{2D} for samples C and F and ungated samples H and G are summarized in Table II. Samples G and F show 4 and 20% decreases, respectively, in N_{2D} after IRQ (no σ_{osc} data is available because of the low mobility of these samples). Samples H and C ($V_g=0$) show 4.5–6.0% decreases in N_{2D} after IRQ. This is accompanied by an increase of 60–100% in the dHS oscillation envelope amplitude at $B=0.8$ T. Notice that the 4.5% decrease of N_{2D} upon ir illumination from sample H is consistent with the 5% decrease in N_s from the Hall measurement establishing the validity of Eq. (1). The *increase* in N_{2D} from ir illumination for sample C with V_g close to V_t will be discussed in Sec. V.

The data show an increase in N_{2D} from white light and then a decrease upon ir illumination. It could be suggested that white light spreads photoexcited electrons from the gap between the gate and Ohmic contacts to under the gate. To avoid a large potential difference along the channel from this hypothetical charge redistribution (which is not observed), N_1 under the gate would have to decrease proportionately. This is contradicted by transconductance measurements that show V_p shifted to more negative values. The conclusion we reach is rather that free carriers are excited in the $Al_xGa_{1-x}As$ layer under the gate upon white-light illumination and then decrease in that region due to infrared illumination.

We will now show how changes in μ_{2D} can be related to changes in the remote ionized donor population due to PPC and IRQ. It has been determined that remote ionized donors in the $Al_xGa_{1-x}As$ layer provide the dominant scattering mechanism of the 2D EG in $GaAs/Al_xGa_{1-x}As$ heterostructures at low temperatures,[5] so that a decrease in N_i reduces scattering and increases the 2D EG mobility. It has also been shown[11,12] that the classical mobility μ_c of the 2D EG obeys the following relation:

$$\mu_c\approx CN_{2D}^{3/2}d_{eff}^3N_i^{-1} . \quad (6)$$

Here, C is a constant and d_{eff} is the effective distance between the ionized donors and the 2D EG determined by the distribution of ionized donors. The 1.5 power relationship between μ_c and N_{2D} is due to screening effects:

TABLE II. Results from dHS oscillation measurements. The percentage change of the 2D electron number densities (N_{2D}) measured after ir (<0.67 eV) illumination from the value of N_{2D} that remains in the PPC state. The percentage change of the dHS oscillation amplitude σ_{osc} after IRQ at $B=0.8$ T. For samples H and C ($V_g=0$) we present the estimated percentage change of ionized donor density N_i in the $Al_xGa_{1-x}As$ layer following ir quenching of the PPC state, the calculated percentage change of 2D EG classical mobility μ_c including screening effects, the calculated percentage change of the quantum lifetime $(\Delta\tau_q/\tau_q)_c$ from the data of μ_c, N_{2D}, and σ_{osc}. The percentage change of quantum lifetime τ_q obtained by fitting the experimental data directly to the leading exponential term is also presented.

	VDP	HEMT			HEMT		
	H	G	F	F	C	C	C
x	0.23	0.30	0.30	0.30	0.21	0.21	0.21
V_g (V)	ungated	ungated	+0.20	0.0	0.0	−1.95	−2.14
$\Delta N_{2D}/N_{2D}$	−4.5%±1%	−4%±2%	−20%±5%	−20%±5%	−6%±2%	+10%±4%	+50%±5%
$\Delta\sigma_{osc}/\sigma_{osc}$	+60%±10%				+100%±10%		
$\Delta N_i/N_i$	−14%±3%				−13%±4%		
$\Delta\mu_c/\mu_c$	+7%±3%				+4%±3%		
$(\Delta\tau_q/\tau_q)_c$	+9%±3%				+16%±8%		
$\Delta\tau_{rvq}/\tau_q$	+6%±2%				+20%±4%		

a decrease of screening by a reduction in N_{2D} enhances the scattering. There are two limiting cases. (i) Near V_t, the relative change of N_{2D} is much bigger than the relative change in N_i and so μ_c decreases with decreasing N_{2D}. (ii) For incomplete depletion of the $Al_xGa_{1-x}As$ layer both N_{2D} and N_i can change. By the depletion approximation and Poisson's equation $N_i \sim N_{2D}^2$. While white light can contribute a fraction α to the total N_{2D} via electron-hole separation in the GaAs buffer layer, ir light has insufficient energy to induce electron-hole recombination in the GaAs buffer layer. Only $(1-\alpha)N_{2D}$ carriers are depleted from the doped $Al_xGa_{1-x}As$ layer by white light and, from the depletion approximation for a fixed conduction-band discontinuity, a small relative change in N_i can be approximated as

$$\Delta N_i/N_i \approx 2(1-\alpha)^{-1}\Delta N_{2D}/N_{2D} . \quad (7)$$

Therefore, for IRQ, the relative decrease in $N_{2D}^{3/2}$ is less than the relative decrease in N_i. Ignoring weak changes in d_{eff}, we observe for incomplete depletion of N_1 that μ_c in Eq. (6) increases when N_{2D} is decreased via IRQ.

The portion α of N_{2D} contributed by electron-hole separation in the GaAs buffer layer may be deduced from the difference between N_{2D} following white light and ir quenching (assuming all photoelectrons originating from traps in the $Al_xGa_{1-x}As$ layer are recaptured after IRQ). For sample H, $\alpha=35\%$, and for sample C ($V_g=0$), $\alpha=10\%$. The resulting estimated values of $\Delta N_i/N_i$ and $\Delta\mu_c/\mu_c$ are shown in Table II.

Two independent methods were used to verify the predicted increase of μ_{2D} in samples H and C ($V_g=0$) both with parallel conductance in the $Al_xGa_{1-x}As$ layer. From Eq. (3), σ_{osc} is an increasing function of both $\sigma_{xx}(B=0)$ and τ_q for fixed magnetic field and temperature. From experimental data showing increases in σ_{osc} after ir quenching and the calculated changes in $\sigma_{xx}(B=0)\approx eN_{2D}\mu_c$, we obtain the changes in τ_q. The results listed as $(\Delta\tau_q/\tau_q)_c$ in Table II indeed show increases for samples H and C ($V_g=0$). The second method directly fits the leading exponential term in Ando's expression to the dHS oscillation data. The results [shown as $(\Delta\tau_q/\tau_q)$ in Table II] also show τ_q increasing after ir illumination. These changes are consistent with the calculated increases of τ_q deduced from σ_{osc}.

In conclusion, dHS oscillations show a decrease in N_{2D} from ir illumination, accompanied by increases in the dHS oscillation amplitude and in τ_q when the $Al_xGa_{1-x}As$ layer is not fully depleted. This suggests ionized traps being filled in the $Al_xGa_{1-x}As$ layer. Together with shifts of V_p during ir illumination, the data indicate that IRQ occurs by the capture of ir-excited free electrons from both the 2D EG and $Al_xGa_{1-x}As$ layer back to ionized donors in the $Al_xGa_{1-x}As$ layer.

IV. CAPTURE CROSS SECTION OF ir-EXCITED ELECTRONS

In the following we use the experimental data to estimate the capture cross sections of ir-excited electrons. It is presumed the ionized donors in the $Al_xGa_{1-x}As$ layer that recapture the carriers are *DX* centers. Under steady infrared illumination, the increase in the density of *occupied DX* centers (N_{DX}) corresponds to a decrease in the free-carrier density, and can be expressed as

$$d(N_{DX})/dt = \sigma(N_{2D0}-N_{DX})(N_{DX0}-N_{DX}) \quad (8)$$

with $\sigma=k(v/l)w$, where k is the trap-capture cross section, v the average z-direction velocity of ir-excited carriers, l is the $Al_xGa_{1-x}As$ layer thickness such that l/v gives the transit time of an ir-excited electron across the $Al_xGa_{1-x}As$ layer, and w is the probability per second of a free carrier being excited by ir illumination of a certain intensity. N_{2D0} is the initial total 2D EG density, such that $(N_{2D0}-N_{DX})$ is the total areal free-carrier density. N_{DX0} is the initial total *unoccupied* areal *DX*-center density at the beginning of an ir quenching interval so that $(N_{DX0}-N_{DX})$ is the unoccupied areal trap density at a given time. A simple single-rate exponential decay would occur when a finite number of carriers were recaptured

by an infinite or very large number of traps, i.e., if $N_{2D0} \ll N_{DX}$. Typically, N_{DX0} is comparable with N_{2D0}, and Eq. (8) is not a simple rate equation, which is consistent with the observed nonexponential decay.

During an infinitesimal time interval δt, the term $(N_{2D0}\text{-}N_{DX})$ may be considered as relatively constant in comparison with $(N_{DX0}\text{-}N_{DX})$, because $N_{2D0} \gg N_{DX0}$. With this in mind $N_{DX}(t_0+\delta t)$ can be obtained from $N_{DX}(t_0)$ and the initial values of N_{2D0} and N_{DX0} by the following approximation:

$$N_{DX}(t_0+\delta t)=N_{DX}(t_0)\exp\{-\sigma[N_{2D0}-N_{DX}(t_0)]\delta t\} + \sigma N_{DX0}[N_{2D0}-N_{DX}(t_0)]\delta t \ . \quad (9)$$

Equation (9) shows that IRQ occurs as a combination of exponential and linear terms. Both terms have decreasing decay rates as the IRQ progresses because N_{DX} increases during decay. The experimental results behave as predicted and the details of the IRQ can be obtained from Eq. (9).

Assuming that all DX centers are unoccupied at $t=0$ (saturated PPC state), calculated values of $[1-N_{DX}(t)/N_{DX0}]$ for $0<t<100$ sec using Eq. (9) are shown in Fig. 7(a), where $N_{2D0}=10\times10^{11}$ cm^{-2}, for two choices of N_{DX0} and three choices of σ. The decay of $[1-N_{DX}(t)/N_{DX0}]$ is shown in Fig. 7(b), with $N_{DX0}=2\times10^{11}$ cm^{-2} while σ and N_{2D0} were varied. Numerical calculations using Eq. (9) show the normalized decay is sensitive to σ and N_{2D0} but not to changes of the estimated value of N_{DX0}. This is expected for $N_{DX0} \ll N_{2D0}$.

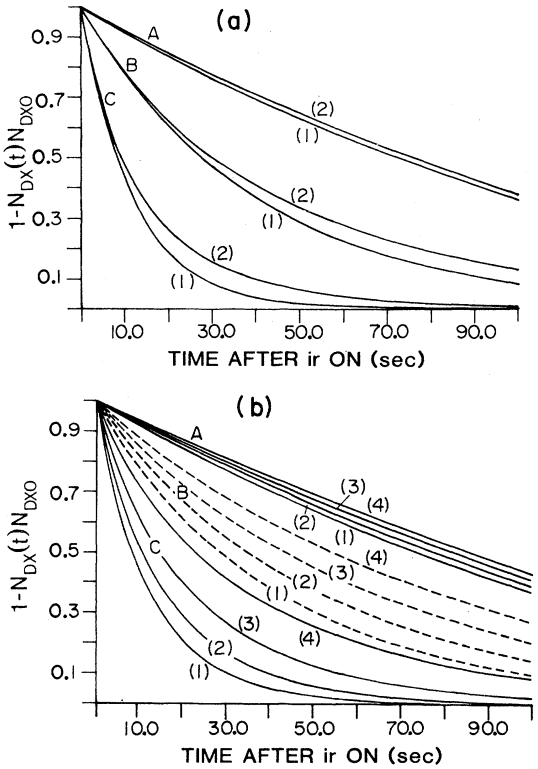

FIG. 7. Theoretical calculation of normalized ir-decay curves (a) shows the weak N_{DX0} dependence [(1) $N_{DX0}=0.5\times10^{11}$ cm^{-2} and (2) $N_{DX0}=5\times10^{11}$ cm^{-2}] but strong σ dependence. σN_{2D0} is fixed at 10×10^{11} cm^{-2}. (b) shows both σ and N_{2D0} are important. N_{DX0} is fixed at 2×10^{11} cm^{-2} and σ and N_{2D0} varied [(1) $N_{2D0}=10^{11}$ cm^{-2}, (2) $N_{2D0}=8\times10^{11}$ cm^{-2}, and (3) $N_{2D0}=6\times10^{11}$ cm^{-2}]. Parameters are chosen to set the values of quenching time close to the experimental range in this work. The values of σ in both (a) and (b) are A, $\sigma=5\times10^{15}$ cm^{-2}; B, $\sigma=2.5\times10^{-14}$ cm^{-2}; C, $=8.5\times10^{-14}$ cm^{-2}.

In order to fit Eq. (9) to the I_{SD} data discussed later, it is necessary to establish the relation between the decay in I_{SD} and the decay of $[1-N_{DX}(t)/N_{DX0}]$, and also determine the N_{2D0} from experimental results. Table III shows results obtained by the methods summarized below.

A. Case i: V_g near threshold (Fig. 4, bottom)

For V_g chosen so as to entirely deplete the free carriers in the $Al_xGa_{1-x}As$ layer, $N_{2D0}-N_{DX}=N_{2D}$. From Eqs. (2) and (6), I_{SD} is considered proportional to $(N_{2D})^{5/2}$ because the relative change in N_i is much smaller than the relative change in N_{2D}. N_{2D0} and N_{DX} are determined by the initial N_{2D} values from dHS oscillations, the I_{SD} data, and the $\frac{5}{2}$ power law relation between I_{SD} and N_{2D}.

B. Case ii: $V_g=0$, parallel conductance dominant (Fig. 4, top)

N_{2D0} and N_{DX} can be estimated for the opposite extreme at $V_g=0$, with parallel conductance in the $Al_xGa_{1-x}As$ layer [$N_1 \gg N_{2D}$, cf. Eq. (2)]. The change in N_{DX} is nearly the same as that in N_1. Since μ_{2D} has been shown to increase when N_{2D} decreases (Table II) during ir quenching, the first term in Eq. (2) for I_{SD} will be essentially constant, and N_1 becomes more important than N_{2D}. The change in I_{SD} during IRQ behaves as a linear function of N_{DX} (since $N_{DX0} \ll N_d$, the change in μ_1 is only weakly dependent on N_{DX} and can be ignored). Before using Eq. (2) to estimate N_1, N_{DX}, and N_{2D0} $(=N_{2D}+N_1$, at $t=0)$ from I_{SD} data, the values of μ_{2D}, N_{2D}, and μ_1 are also needed. N_{2D} $(=8\times10^{11}$ cm$^{-2})$ is directly measured from dHS oscillations. The value of μ_{2D} $(=2.2\times10^4$ cm^2/V sec) is directly measured on sample B ($V_g=0$) by the geometric-magneto-transconductance (GMT) method[3,13] and the value of μ_1 is estimated[4] to be 0.1×10^4 cm^2/V sec. For sample B at 77 K, N_{DX0} at $V_g=0$ is about 2.3×10^{11} cm^{-2}, corresponding to a bulk density of 2.3×10^{16} cm^{-3}, which is much smaller than N_d, and the change in μ_1 can be ignored during ir quenching.

TABLE III. Effective ir-quenching capture cross sections. The estimated value of N_{2D0} (initial total 2D EG number density), or effective N_{2D0} (Ref. 14) and N_{DX0} (initial *unoccupied DX*-center density) of sample B at 77 K (with different gate biases). These were obtained as the sample approached the PPC baseline following a short 1.4-eV light exposure but (see Figs. 2 or 3) before ir ($h\nu < 0.67$ eV) quenching. All densities are in units of 10^{11} cm^{-2}. The fitting values of σN_{2D0} and estimated values of σ ($=kv/lw$) are also presented. The units of σN_{2D0} are sec^{-1}, and the units of σ are 10^{-15} sec^{-1}/cm^2. Even with the variation from the choice of N_{2D0} or effective N_{2D0} an order of magnitude value of σ was determined.

V_g (V)	N_{2D0}	Effective N_{2D0}	N_{DX0}	σN_{2D0}	σ
0	24±4	24	2.4±0.4	0.02±0.005	6–10
−0.15	15±4	24	2.4±0.4	0.02±0.005	6–20
−0.30	7.6±2	24	2.3±0.4	0.03±0.005	12–40
−0.40	6.4±1	24	2.3±0.4	0.03±0.005	12–47
−0.50	2.4±0.4	24	1.5±0.4	0.04±0.01	17–170

C. Case iii: Intermediate situation, $V_p < V_g < 0$ (Fig. 4, middle)

V_g does not change N_{2D} when the $Al_xGa_{1-x}As$ layer is not entirely depleted ($V_g > -0.38$ V for sample B).[3] For $V_g = 0$, -0.4, and -0.5 V (Table III) N_{DX0} has a weak gate-bias dependence until V_g is near V_t and rapid band bending in the $Al_xGa_{1-x}As$ layer narrows the region where IRQ occurs. The agreement in estimated values for N_{DX0} indicates that the assumed relation between I_{SD} and the carriers in different layers versus V_g is a good approximation. The values of N_{DX0} for $V_g = -0.15$ and -0.30 V which are mixed situations (carriers in the $Al_xGa_{1-x}As$ layer and also in the 2D EG) are obtained by linear interpolation. The initial value of N_{2D0} for $V_g = -0.15$ V is the same as for $V_g = 0$, but in when $V_g = -0.30$ V (and $V_g > V_p = -0.28$ V) after IRQ, the $I_{SD} \sim N_{2D}^{5/2}$ power-law relation was used. These results for sample B are summaried in Table III.

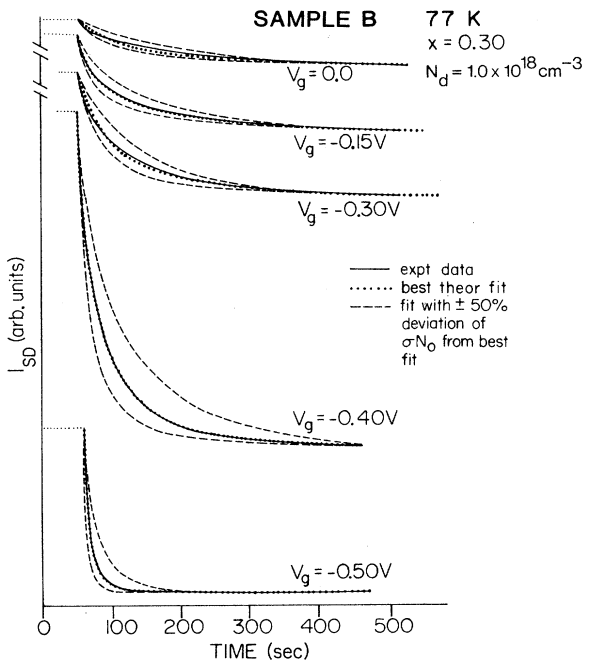

FIG. 8. The theoretical fitting of the ir-quenching data from sample B at 77 K by Eq. (4) using N_{2D0} and N_{DX0} from Table III. The results of σ ($=kv/lw$) are shown in Table III. In addition, Eq. (4) is plotted using values of σN_{2D0} that are ±50% of the best fit values. The I_{SD} data for different gate biases is not shown in same scale, and the I_{SD} zero has been offset for better observation.

Knowing the relation between I_{SD} and N_{DX}, the fit of Eq. (9) to experimental data of sample B at 77 K versus V_g (Fig. 8) gives values of σN_{2D0} and σ that are summarized in Table III. The excellent agreement with experiment for this very nonexponential decay is strong evidence for the validity of the theory of Eq. (9). The decay curves of I_{SD} that are calculated using σN_{2D0} with a 50% deviation from the best-fit values are also presented in Fig. 8. Because the decay is very sensitive to the choice of σN_{2D0} (Fig. 7), variations such as those due to changes in the power law between I_{SD} and are N_{DX} neglected. Although there is a big difference between N_{2D0} and the so-called effective N_{2D0} as V_g approaches V_t it is sufficient to obtain the magnitude of σ, which is on the order of 10^{-14} sec^{-1} cm^2.

Applying this analysis to sample D yields similar values of σ. By fitting Eq. (9) to the ir-quenching curve of N_s from sample D (Fig. 2), and for simplicity, considering that N_s is a linear function of N_{DX}, we obtain $\sigma N_{2D0} = 0.03$ sec^{-1} with $N_{2D0} \approx 1 \times 10^{12}$ cm^{-2} including N_1 in the parallel conductance layer. The value of σ for sample D is also on the order of 10^{-14} sec^{-1} cm^2.

D. Absolute ir capture cross section

The ir-light source was a quasiblackbody lamp filtered through a germanium filter with an intensity of $\sim 10^{12}$ photons sec^{-1} cm^{-2} at the sample. The ir-absorption cross section of free electrons is about 10^{-19} cm^2 in this experiment (see Appendix), so only 1 in 10^7 of the free photoelectrons per second are active in the retrapping process. The dependence on V_g of the length l over which the ir-excited electrons move may be neglected. For example, the distance from the 2D EG to the far end

of the undepleted $Al_xGa_{1-x}As$ layer is 40 nm for $V_g=-0.40$ V and 50 nm for $V_g=0$. This difference makes a negligible contribution to the enhancement of σ. Using $v\approx 10^8$ cm/sec (an electron with 0.1–0.5 eV of energy), $l=10^{-5}$ cm and $\sigma[=k_{ir}(v/l)w]\sim 10^{-14}$ $sec^{-1}cm^2$, the absolute ir capture cross section, k_{ir} should be on the order of 10^{-20} cm^2. This result for k_{ir} is much smaller than the trap size (about 10^{-15} cm^{-2}) in the $Al_xGa_{1-x}As$ layer, and consistent with the existence of a capture barrier. However, k_{ir} is much larger than the thermal capture cross section (k_T) detected at the same temperature. An estimate of k_T can be reached using $k_T\approx 1/(Nv\tau)$. Reference 14 shows that for $x=0.3$ the thermal capture lifetime, $\tau\approx 1$ sec at 77 K with a thermal prefactor of 10^{-11} sec, and the *DX*-center capture barrier to be about 150 meV). Using a carrier number density $N\approx 10^{18}$ cm^{-3} (same order as doping density), $v\approx 10^8$ cm/sec and $\tau=1$ sec, we find $k_T\approx 10^{-26}$ cm^2 which is consistent with other reported results.[15] The capture lifetime at a higher temperature corresponds to that of an electron with a larger energy, which is consistent with IRQ because of the much higher effective temperature ($T\approx 10^3$ K) of the ir-excited electrons. This capture cross section enhancement by a factor of 10^6 from ir illumination should be considered in reasonable agreement with the results of thermal capture experiments. Our ir-quenching time constants at $T=2$–4 and 30 K show *no significant difference* from the values determined at $T=77$ K for the same sample and gate biases. The temperature independence of the capture cross section is further evidence of the high-energy temperature-independent behavior of the ir-excited electrons.

V. GATE-BIAS DEPENDENCE OF INFRARED QUENCHING

For certain conditions of gate bias we have observed IRQ occurring at energies as low as 0.5 eV and as high as to 1.2 eV (samples B and F). We propose variation in optical threshold is due to internal electric fields (**E**) which effect the photo threshold of the deep centers. It is possible in gated samples to vary **E** in the $Al_xGa_{1-x}As$ layer, with **E** being strongest at the GaAs-cap–$Al_xGa_{1-x}As$ interface (see Fig. 4). Using parameters in Table I and Poisson's equation, the maximum value of **E** at the interface between the GaAs cap and $Al_xGa_{1-x}As$ layer can be calculated for a given V_g. Samples with a maximum $E<2\times 10^5$ V/cm show strong IRQ (Table II). When V_g approaches V_t for sample C (which has a low threshold voltage, $V_t=-2.4$ V after PPC), IRQ weakens until $E\sim 3\times 10^5$ V/cm ($V_g=-1.6$ V) in the $Al_xGa_{1-x}As$ layer, after which ir light *increases* I_{SD} significantly (Fig. 9). This is observed over the entire temperature range $2<T<77$ K. dHS measurements confirm this is due to an increase of N_{2D} (shown also in Table II).

Figure 10 shows that for the proper choice of V_g (Fig. 4, bottom) ir illumination also *enhances* I_{SD}. The intervals A–D in Fig. 10 show strikingly different rise times to ir illumination depending on net light exposure history for this region of V_g near pinchoff. The data show when the sample has been cooled down in the dark (A), or I_{SD} is near the in-dark value following a long decay interval (D), the rise time is slower than at other times (B,C) in its light exposure history. A depletion calculation (analogous to the differences shown in Fig. 4 from top to bottom), for cases A and D shows that band bending in the doped $Al_xGa_{1-x}As$ layer is much less steep (and E is smaller) than right after white light has been removed. This may explain the slow rise times for these cases. On

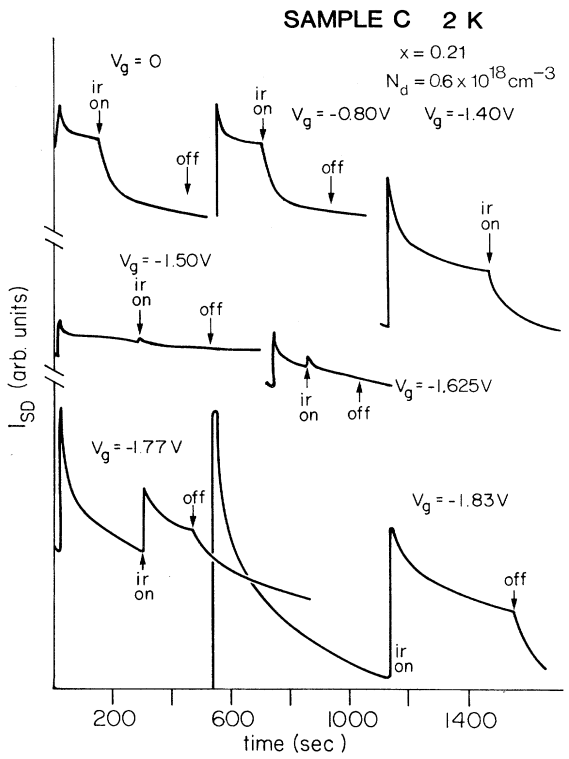

FIG. 9. Gate-bias dependence of ir quenching from sample C with $x=0.21$. When V_g approaches threshold, the ir quenching weakens until the maximum electric field in the $Al_xGa_{1-x}As$ layer is about 3×10^5 V/cm ($V_g=-1.5$ V), after which the ir light actually *increases* the conductivity.

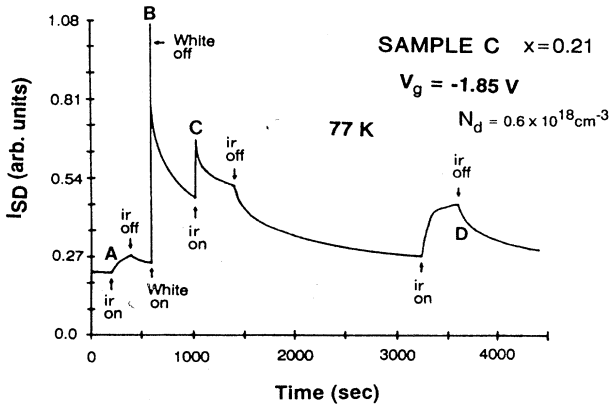

FIG. 10. The ir enhancement with different illumination and decay histories from sample C with $V_g=1.85$V. A–D mark strikingly different rise times to ir illumination depending on net light exposure history for this range of V_g near pinchoff.

the other hand, the slow rise time is not observed when V_g is further from V_t (Fig. 9). An investigation of these results will be left for future work.

In all cases, these ir (or more precisely, the high-energy portion of ir induced *enhancements* of I_{SD} decay with a lifetime of 10^2 sec (for both $T=2$ and 77 K) after the ir light is turned off. This decay is much faster than the typical *DX*-center-related PPC decay (hours to days) at the same temperatures.

A change in the emission rate of trapped electrons due to the Frenkel-Poole effect and phonon-assisted tunneling has been shown to be important in the strong electric field of a heavily doped junction.[16] One such deep trap (the EL2 level in GaAs) with a gate-bias-dependent emission rate has been shown to have *DX*-center-type behavior.[17] For these *DX*-center-like traps (Fig. 11), strong electric fields may also change the energy difference between different configurations. When the microscopic orientation of the *DX* center is favorable, the shift of emission energy from $E_{e,1}$ to $E_{e,2}$ in Fig. 11 (by a change in the applied electric field) must be accompanied by a shift in capture energy from $E_{c,1}$ to $E_{c,2}$, as well as the onset optical threshold from $E_{\mathrm{op},1}$ to $E_{\mathrm{op},2}$. This decrease in the onset optical threshold can explain the change from ir quenching to ir enhancement. The smaller capture energy barrier (or larger capture cross section) under a strong electric field is consistent with the V_g-dependent results of k_{ir} (Table III). But the E-field dependence of the configuration energy of *DX*-center traps is not clear and more detailed experiments should be undertaken in order to understand this in terms of the various models raised for *DX* centers.

When sample C has all its traps in the $Al_xGa_{1-x}As$ layer emptied by cooling down from 300 K at $V_g < V_t$ (at 300 K),[14] the value of V_t at 77 K (-4.0 V) is the same as that at 300 K. In this case ($T=77$ K) there is significant IRQ for $V_g > -3.0$ V, but there is no change in I_{SD} (neither enhancement nor quenching) observed from ir illumination after white light (no PPC effect either) when V_g is set close to V_t because of an absence of trapped electrons. This phenomenon provides additional evidence that under very strong electric fields the emptied traps in the $Al_xGa_{1-x}As$ layer do not capture free electrons.

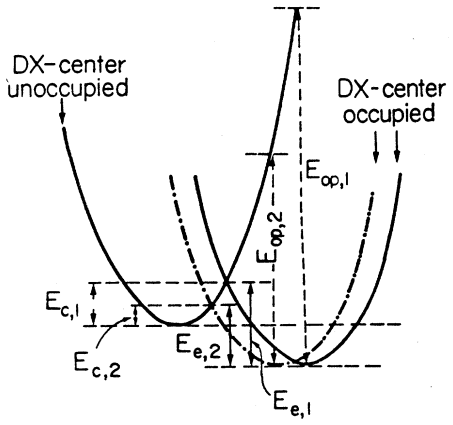

FIG. 11. The proposed electric-field effect on the *DX* centers.

VI. SUMMARY AND FUTURE WORK

This work investigates *DX*-center-related ir quenching via carrier number density and conductance measurements on $GaAs/Al_xGa_{1-x}As$ heterostructures at $2 < T < 77$ K. The study was carried out on a variety of gated and ungated samples from different sources. We confirm that, after brief white-light exposure to induce the persistent photocurrent state, infrared (ir, $h\nu < 0.7$ eV) illumination induces quenching of PPC on ungated samples or gated samples at small gate biases. The commonality of results among these show that the IRQ effect is the same over a range of Al fraction, spacer layer thickness, doping levels, and threshold voltages (see Table I).

Measurements of dHS oscillations show a decrease of the 2D EG number density after ir illumination, accompanied by increases in the dHS oscillation amplitude and the carrier scattering lifetime when the $Al_xGa_{1-x}As$ layer is not fully depleted. This suggests that ir light fills ionized traps in the $Al_xGa_{1-x}As$ layer, which are believed to be the main scattering centers. Together with shifts of the transconductance peak during ir quenching, the data indicate that the quenching is dominated by capture of ir-excited free electrons back to deep centers in the $Al_xGa_{1-x}As$ layer. The ir-quenching times at $2 < T < 77$ K are *temperature independent.* The ir capture cross section is estimated to be on the order of 10^{-20} cm^{-2}. This result is reasonable considering the energy of ir-excited free electrons and the deep-trap-capture barrier height and decay prefactor.

Experiments on a sample with a higher internal electric field ($> 3\times10^5$ V/cm) from V_g show a *strong* increase in the conductivity with the same ir illumination. This E-field dependence of the optical threshold may be due to a change in the trap configuration energy under a strong electric field. More detailed experiments, for example, on the electric-field dependence of the emission barrier from the same traps in the $Al_xGa_{1-x}As$ layer, and the ir photon-energy dependence of the capture cross section of ir quenching, should be undertaken to choose between various models for *DX* centers.

ACKNOWLEDGMENTS

The authors would like to thank R. Gleason and R. Koyama (Tektronix); P. R. Jay and P. Delescluse (Thomson-CSF); W. Schaff (Cornell); and S. C. Palmateer (General Electric) for providing the samples used in this study. This work was supported in part by the Tektronix Foundation and the National Science Foundation through Grant No. DMR85-19728.

APPENDIX

The infrared light in most of this work came from a tungsten lamp passing through a germanium filter with a cutoff energy at 0.67 eV. The tungsten lamp was treated as a quasiblackbody with 10–20 % efficiency and a maximum spectral emittance at 1 μm. About 20% of the to-

tal emitted energy occurs in the 2–5-μm range. For an estimated input power of 10 W to the lamp there should be ~ 0.1 W of infrared (2–5 μm) output. Finally, there was an additional factor-of-10 intensity attenuation from the Ge filter and glass dewar walls.

Theory and experiments have shown[18] that free-carrier absorption coefficient in a semiconductor is proportional to the free-carrier number density, and is inversely proportional to the conductivity mobility. For the near-infrared light (2–5 μm) in this work, the free-electron absorption coefficient is also proportional to the cube of the free-space wavelength when impurity scattering is dominant. From the experimental data on a Te-doped GaAs sample,[19] the absorption coefficient is measured to be about 1 cm^{-1} at 80 K for a free-electron number density $\approx 1 \times 10^{18}$ cm^{-3}. This gives a free-carrier absorption cross section on the order of 10^{-18} cm^2. For the MBE-grown samples in this work with free-carrier mobilities larger by a factor of 10, the free-electron absorption cross section is estimated to be on the order of 10^{-19} cm^2.

[1]M. I. Nathan, T. N. Jackson, P. D. Kirchner, E. E. Mendez, G. D. Pettit, and J. M. Woodall, J. Electron. Mater. **12**, 719 (1983); L. X. He, K. P. Martin, and R. J. Higgins, Bull. Am. Phys. Soc. **31**, 656 (1986).

[2]R. J. Nelson, Appl. Phys. Lett. **31**, 351 (1977).

[3]J. P. Harrang, R. J. Higgins. R. K. Goodall, R. H. Wallis, P. R. Jay, and P. Delescluse, J. Appl. Phys. **58**, 4431 (1985).

[4]T. J. Drummond, W. T. Masselink, and H. Morkoç, Proc. IEEE **74**, 777 (1986).

[5]J. P. Harrang, R. J. Higgins, R. K. Goodall, P. R. Jay, M. Laviron, and P. Delescluse, Phys. Rev. B **32**, 8126 (1985).

[6]J. P. Harrang, Ph.D. dissertation, University of Oregon, 1984 (unpublished).

[7]T. J. Drummond, W. Kopp, R. Fischer, H. Morkoç, R. E. Thorne, and A. Y. Cho, J. Appl. Phys. **53**, 1238 (1982).

[8]T. Ando, J. Phys. Soc. Jpn. **37**, 1233 (1974).

[9]D. W. Terwilliger and R. J. Higgins, Phys. Rev. B **7**, 667 (1973).

[10]A. C. Beer, *Galvanomagnetic Effects in Semiconductors* (Academic, New York, 1963), Vol. 71.

[11]P. J. Price, Surf. Sci. **113**, 199 (1982).

[12]K. Lee, M. S. Shur, T. J. Drummond, and H. Morkoç, J. Appl. Phys. **54**, 6432 (1983).

[13]P. R. Jay and R. H. Wallis, IEEE Trans. Electron Devices Lett. **2**, 265 (1981).

[14]P. M. Mooney, N. S. Caswell, P. M. Solomon, and S. L. Wright, in *Microscopic Identity of Electronic Defects in Semiconductors,* MRS Conf. Proc. No. 46, edited by Noble M. Jackson, Stephen G. Bishop, and George B. Watkins (MRS, Pittsburgh, 1985), p. 403.

[15]P. M. Mooney, P. M. Solomon, and T. N. Theis, in *International Symposium GaAs and Related Compounds,* edited by B. de Cremoux, IOP Conf. Proc. No. 74 (IOP, Bristol, 1985), Chap. 7.

[16]G. Vincent, A. Chantre, and D. Bois, J. Appl. Phys. **50**, 5484 (1979).

[17]G. Vincent, D. Bois, and A. Chantre, J. Appl. Phys. **53**, 3643 (1982).

[18]B. A. Smith, *Semiconductors* (Cambridge University, London, 1978), p. 294.

[19]I. Balslev, Phys. Rev. **173**, 762 (1968).